Available online at www.sciencedirect.com
SCIENCE DIRECT
ELSEVIER
European Journal of Mechanics B/Fluids 23 (2004) 797–813
EUROPEAN JOURNAL OF MECHANICS B/FLUIDS

The evolution of free-disturbances in a two-dimensional nonlinear critical layer

T. Allen

Met Office, FitzRoy Road, Exeter, EX1 3PB, England, UK

Received 26 June 2003; received in revised form 2 March 2004; accepted 2 April 2004

Available online 29 July 2004

Abstract

This paper investigates the evolution of (relatively) long Rayleigh waves on an inflectional two-dimensional boundary layer such as may occur when a flow encounters a small surface mounted obstacle. Under the assumption that the flow remains essentially two-dimensional a coupled set of evolution equations are derived that describe the nonlinear growth of an essentially arbitrary (2D) disturbance to the base flow. Numerical solutions are presented for a representative initial condition.

Keywords: Critical layer; Triple-deck; Rayleigh waves; Vortex roll-up

1. Introduction

In a recent series of papers Savin et al. [1], Allen et al. [2] and Allen [3] the nonlinear development of long Rayleigh waves on an inflectional boundary layer flow was investigated. The analysis in these papers is based upon the high Reynolds number asymptotic analysis of flow over small surface mounted obstacles which was first studied by Smith [4] and later further elucidated in Smith et al. [5]. The stability of such flows has been considered by Tutty and Cowley [6] and Smith and Bodonyi [7] wherein it was shown that the appropriate scales for the development of an inflectional sublayer were $O(R^{-1/2}h)$ in the direction normal to the wall and $O(h^3)$ in the streamwise direction. Here $R \gg 1$ is the Reynolds number and h is an asymptotically small height parameter which is equal to $R^{-1/8}$ in the now classical triple-deck theory (see for example the reviews of Stewartson [8] and Smith [9]) but can take values in the range

$$R^{-1/4} \ll h \leqslant R^{-1/8}, \tag{1}$$

where the lower limit corresponds to the case where the lateral and transverse length scales are comparable and hence results in the full Navier–Stokes equations with unit Reynolds number.

An important aspect of the work of [1] was the observation that, by studying relatively long wavelengths near to the onset of the inflectional profile, initial disturbances of an essentially arbitrary character could be incorporated into the nonlinear stability analysis with a Fourier transform replacing the usual modal analysis. A similar property was exploited in Chapman and Proctor [10] for the onset of thermal convection between poorly conducting walls although the nature of the nonlinear interactions are quite different. The work of Gaster [11] and Gaster and Grant [12] is worth mentioning in this context. In these papers the Orr–Sommerfeld equation was solved as an initial value problem and the evolution of the resulting wave packet was compared with experimental results. Although the results were rather favourable the use of the so-called parallel flow approximation instead of the more rational asymptotic approach makes their theory difficult to generalize to include flow development and nonlinearity.

E-mail address: thomas.allen@metoffice.com (T. Allen).

0997-7546/$ – see front matter
doi:10.1016/j.euromechflu.2004.04.005

The importance of the type of disturbance considered here and in [1–3] is made clear in the experiments of Klebanoff and Tidstrom [13] where it was observed that roughness induced disturbances which grow and induce transition involve all frequencies and were not of the fixed frequency type usually investigated in stability theory. Kendall [14] has examined the evolution of a disturbance produced by an isolated element and found that long lived elongated vortical structures exist downstream of the element. It appears possible that the present work describes, at least in their earlier stages of development, these vortices. Other examples of experiments of these types of flow can be found in [15–19] along with the review article of Morkovin [20] and the album of Van Dyke [21].

The present work differs from that of [1–3] in that it is concerned with disturbances which are strictly two-dimensional while the earlier analyses all considered three-dimensional perturbations. The consequence of this difference is that the jump across the critical layer can no longer be calculated explicitly but must be obtained by solving the nonlinear critical layer equations with coupling to the outer (core) flow. The surprising fact that the two-dimensional problem cannot be solved while the three-dimensional one can arises from the change in nature of the critical level singularity as noted by Goldstein and Choi [22], Wu and Cowley [23] and Wu et al. [24]. The difference arises from the fact that the logarithmic singularity in two dimensions spawns a pole singularity in three dimensions and this changes the balance of nonlinear terms within the critical layer which then allows an exact solution to be obtained. This fact was actually first observed and exploited in the study of singular neutral eigenmodes of the Kuo equation by Hickernell [25].

Previous studies of two-dimensional critical layers which followed on from the seminal work of Stewartson [26] (see the reviews of Stewartson [27] and Maslowe [28] for further references) have all considered periodic disturbances. Of particular relevance to the present study are the papers Goldstein and his co-workers [29–32] wherein high Reynolds number asymptotics were used to derive the equations governing the evolution of nonlinear Rayleigh waves in a mixing layer which is far, based upon scales large compared to the wave amplitude, from neutrality. The amplitude equations derived in these papers, which are very similar to the ones derived herein, were used to investigate the roll-up of vorticity within the critical level into "cat's eyes". The removal of the periodicity constraint in the present work means that formation and roll-up of only a finite number of vortices can be described. This is much closer to what one would expect to observe experimentally where an infinite series of periodic vortices will not form immediately downstream of the roughness element but will take a finite time to appear as the initial disturbance rolls up and moves downstream.

The structure of the paper is as follows. In Section 2 a brief description of the equations and scalings will be given. The amplitude equations are then derived in Section 3 with the numerical scheme used to solve them summarised in Section 4. The results of some representative simulations are then described in Section 5 followed by a brief discussion in Section 6 which concludes the paper.

2. Equations and scalings

The nondimensional incompressible Navier Stokes equations are

$$\begin{aligned} &u_t + uu_x + vu_y = -p_x + R^{-1}(u_{xx} + u_{yy}),\\ &v_t + uv_x + vv_y = -p_y + R^{-1}(v_{xx} + v_{yy}),\\ &u_x + v_y = 0, \end{aligned} \tag{2}$$

where (u, v) are the streamwise (x) and transverse (y) velocity components, t is time, p is the pressure and $R = UL/\nu$ is the large scale Reynolds number based upon a suitable velocity scale U, length scale L and the kinematic viscosity ν.

As explained in the introduction and shown schematically in Fig. 1, it is envisaged that the oncoming boundary layer encounters a small surface roughness of height $O(R^{-1/2}h)$ and horizontal extent $O(h^3)$ and so, following [2], the scalings

$$x = h^3\bar{x}, \quad t = h^2\bar{t}, \quad y = R^{-1/2}h\bar{y}, \quad (u, v) = h(\bar{u}, \bar{v}), \quad p = h^2\bar{p}, \tag{3}$$

are introduced. These scalings follow from those used in the lower deck of the now classical triple-deck theory of Stewartson [33] and Messiter [34] and are described in [5] for the present flow configuration. Substitution of (3) into (2) gives upon dropping the bars

$$\begin{aligned} &u_t + uu_x + \epsilon^{-6}vu_y = -p_x + + u_{yy} + \epsilon^{12}u_{xx},\\ &v_t + uv_x + \epsilon^{-6}vv_y = -\epsilon^{-6}p_y + + v_{yy} + \epsilon^{12}v_{xx},\\ &u_x + \epsilon^{-6}v_y = 0, \end{aligned} \tag{4}$$

where $\epsilon = R^{-1/12}h^{-1/3}$ ($\ll 1$). From this definition of ϵ it can be seen that the lower limit upon h in (1) corresponds to the case $\epsilon = 1$.

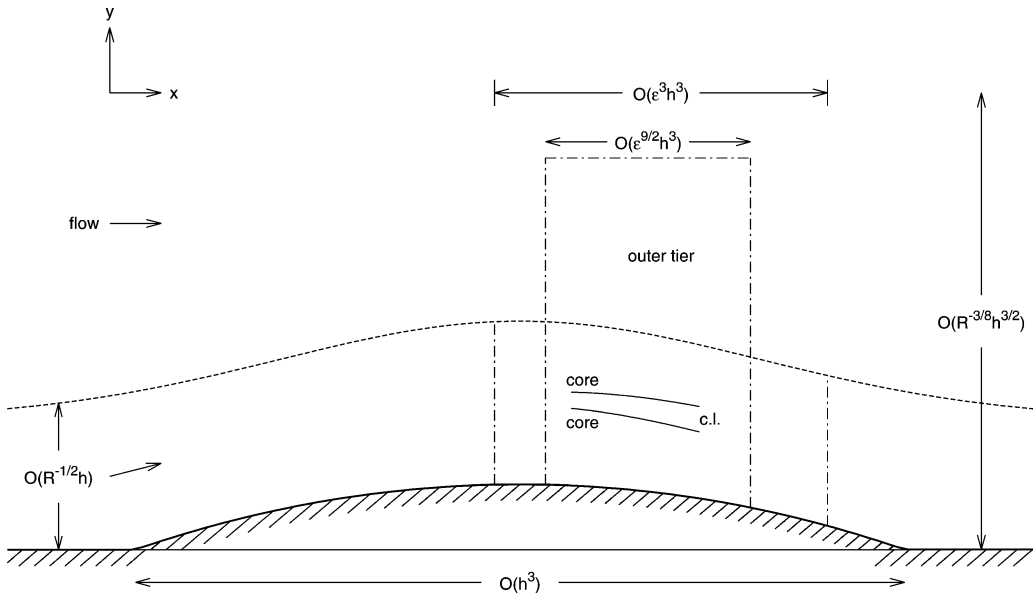

Fig. 1. Schematic showing the geometry of the flow. Here c.l. is the critical layer.

Following [1–3] the fast (long) Rayleigh scales

$$(X,T)=\epsilon^{-9/2}(x,t), \qquad (x_1,t_1)=\epsilon^{3/2}(X,T)=\epsilon^{-3}(x,t), \tag{5}$$

are introduced. Here the X scale is the short length scale upon which the disturbance is described while T is the corresponding time scale over which it propagates. The longer scales (x_1, t_1) represent the modulation scales over which the disturbance grows and are linked to the growth rate of the instability.

The choice of scalings (5) is explained in detail in [1,2]. A brief explanation is as follows. In order to obtain the Rayleigh equation from (4) the wavenumber, α say, must be large of order $\epsilon^{-6}\sigma$ where σ is a measure of the comparative smallness of the wavenumber.[1] Within the critical layer, of thickness μ, the mean velocity is linear and so the term $u\partial_x$ is $\mathrm{O}(\epsilon^{-6}\mu\sigma)$ while the viscous term is $\mathrm{O}(\mu^{-2})$. Balancing these terms then leads to the relation $\sigma\mu^3=\epsilon^6$ which yields, on assuming the reduced wavenumber is comparable the critical layer thickness,[2] $\sigma=\mu=\epsilon^{3/2}$ and hence the scalings (5).

In the following the mean flow $U_0(y)$ is assumed to possess the following properties:-

$$U\sim y \quad \text{as } y\to\infty, \qquad U-c_0=0=U_0'' \quad \text{at } y=y_c, \tag{6}$$

and

$$\fint_0^\infty \frac{\mathrm{d}y}{[U_0-c_0]^2}=0, \tag{7}$$

along with the obvious no-slip condition $U_0(0)=0$. Here the double bar on the integral sign signifies that it is to be interpreted as a Hadamard finite part. The first of conditions (6) comes from the fact that the flow under consideration arises from the lower-deck of the triple-deck structure while the second is simply the condition that the mean flow possesses an inflection point. The final condition (7) determines the velocity c_0 at the critical level and will be derived in the following section. It is interesting to observe that the integral constraint (7) has been found to apply, after a suggestion by Smith [35], to separation/instability of planar interacting boundary layers as shown in Peridier et al. [36], Hoyle et al. [37] and Cassel et al. [38]. A condition similar to (7) also appears in the theory of dispersive surface gravity waves on a sheared current (see for example Johnson [39]) where it is referred to as the Burns condition.

[1] The present analysis is based around the long wave limit of the Rayleigh equation and so $\sigma \ll 1$ is a measure of the smallness of the wavenumber.

[2] This ensures that the expansion proceeds in powers of the single parameter σ.

3. Derivation of the amplitude equations

In accordance with the analysis of [1–3] the lower deck flow structure splits into three asymptotic regions; an inner core (which is the bulk of the lower-deck), an outer core required to satisfy decay in the far field and a critical layer which is required to smooth out the induced logarithmic jump in the velocity.

These regions will be described in the following subsections with the interested reader referred to [1,2] for a detailed derivation of the scalings used.

3.1. The outer core

Since solutions of the Rayleigh equation decay with height on length scales comparable to the horizontal wavelength (see Drazin and Reid [40], p. 143) which is of relative order $\epsilon^{-3/2}$ in the present analysis it follows that $\tilde{y} = \epsilon^{3/2} y = \mathrm{O}(1)$ is the natural vertical coordinate in this region and so the expansion takes the form

$$\begin{aligned} u &= \epsilon^{-3/2}\tilde{y} + \cdots + \delta[\tilde{u}_0 + \epsilon^{3/2}\tilde{u}_1 + \cdots], \\ v &= \cdots + \delta[\tilde{v}_0 + \epsilon^{3/2}\tilde{v}_1 + \cdots], \\ p &= \cdots + \epsilon^{-3/2}\delta[\tilde{p}_0 + \epsilon^{3/2}\tilde{p}_1 + \cdots], \end{aligned} \tag{8}$$

where δ is a small parameter which is determined by the requirement that the jump across the critical level is nonlinear.

Substitution of (8) into (4) using the scalings (5) shows that at leading order the vertical velocity satisfies the Laplace equation,

$$\frac{\partial^2 \tilde{v}_0}{\partial X^2} + \frac{\partial^2 \tilde{v}_0}{\partial \tilde{y}^2} = 0, \tag{9}$$

which is to be solved subject to decay at large distances plus matching to the inner core as $\tilde{y} \to 0$.

Writing

$$\tilde{v}_0 = -A_X \quad \text{on } \tilde{y} = 0, \tag{10}$$

in anticipation of the results from the inner core leads to the solution

$$\tilde{v}_0 = -\frac{\tilde{y}}{\pi} \int_{-\infty}^{\infty} A_\xi(\xi, T, t_1, x_1) \frac{\mathrm{d}\xi}{(X-\xi)^2 + \tilde{y}^2}, \tag{11}$$

from which it follows, for later use, that

$$\left.\frac{\partial \tilde{v}_0}{\partial \tilde{y}}\right|_{\tilde{y}=0} = \frac{1}{\pi} \barint_{-\infty}^{\infty} A_{\xi\xi}(\xi, T, t_1, x_1) \frac{\mathrm{d}\xi}{X-\xi} \equiv G_{\mathrm{Outer}}, \tag{12}$$

where the bar on the integral sign signifies that it is to be interpreted as a Cauchy principal value.

3.2. The inner core

In this region y is O(1) while the disturbance perturbation to u is larger by a factor of $\epsilon^{-3/2}$. The expansion (8) is thus replaced by

$$\begin{aligned} u &= U_0(y) + \epsilon^{3/2} U_1(y) + \cdots + \epsilon^{-3/2}\delta[u_0 + \epsilon^{3/2} u_1 + \cdots], \\ v &= \cdots + \delta[v_0 + \epsilon^{3/2} v_1 + \cdots], \\ p &= \cdots + \epsilon^{-3/2}\delta[p_0 + \epsilon^{3/2} p_1 + \cdots], \end{aligned} \tag{13}$$

where U_1 is the perturbation to the mean (inflectional) flow U_0 arising from the spatial development of the flow; i.e. the Taylor expansion about a point (upstream or downstream) of distance $\mathrm{O}(\epsilon^{3/2})$ from the inflection point. Note that nonparallel terms first occur at $\mathrm{O}(\epsilon^3)$ in this expansion and so do not contribute to the analysis in this region.

Substituting this expansion into (4) and changing to a coordinate system moving at the inflectional speed ($\partial/\partial T \equiv -c_0 \partial/\partial X$) gives (see [2,3]) the lead order solution

$$v_0 = A_X(U_0 - c_0)\int_{\infty}^{y} \frac{\mathrm{d}z}{[U_0(z) - c_0]^2}, \tag{14}$$

for $y > y_c$ while the solution below the critical level ($y < y_c$) has the lower limit of integration replaced by zero. Continuity at $y = y_c$ now leads to the constraint (7).

The solvability condition for the critical layer is obtained at next order in the expansion where the solution is

$$v_1 = (U_0 - c_0)\left(\int_{\infty}^{y} \frac{G\,\mathrm{d}z}{[U_0(z) - c_0]^2} + G_{\text{Outer}}\right), \tag{15}$$

for $y > y_c$ with the solution in $y < y_c$ obtained by replacing the lower limit of integration by zero and neglecting the term G_{Outer} which arises from matching to the outer core (12). The function G in (15) is

$$G = p_{1X} + p_{0x_1} - (U_0 - c_0)u_{0x_1} + u_{0t_1} + U_0 u_{0x_1} + U_1' v_0 - U_1 v_{0y}, \tag{16}$$

which it transpires is regular at the critical level $y = y_c$. The jump across the critical level is determined by the difference in the coefficient of $(y - y_c)$ in the Taylor expansion of v_1 from above (G_R^+) and below (G_R^-) the critical level. From (15) it now follows that

$$G_R^+ - G_R^- = b_1 G_{\text{Outer}} - b_1 \fint_{0}^{\infty} \frac{G\,\mathrm{d}y}{[U_0 - c_0]^2}, \tag{17}$$

where $b_1 = U_0'(y_c) > 0$ is the shear at the critical level height. After some working it follows that the integrand in (17) can be written as (using $p_0 \equiv A$)

$$\fint_{0}^{\infty} \frac{G\,\mathrm{d}y}{[U_0 - c_0]^2} = -2\left\{J_1\frac{\partial}{\partial t_1} + c_0 J_1\frac{\partial}{\partial x_1} + J_2\frac{\partial}{\partial X}\right\}A, \tag{18}$$

where the constants $J_{1,2}$ are determined from the integrals

$$J_1 = \fint_{0}^{\infty} \frac{\mathrm{d}y}{[U_0 - c_0]^3}, \qquad J_2 = \fint_{0}^{\infty} \frac{U_1\,\mathrm{d}y}{[U_0 - c_0]^3}, \tag{19}$$

which are completely determined by the oncoming interactive boundary layer.

3.3. The critical layer

Within the critical layer, whose thickness is $\mathrm{O}(\epsilon^{3/2})$, the stretched coordinate $Y = \epsilon^{-3/2}(y - y_c) = \mathrm{O}(1)$ is introduced with the value of δ now fixed by the requirement that the critical layer jump is nonlinear. To achieve this it is observed that the critical layer is being matched to a term of $\mathrm{O}(\epsilon^3\delta)$ in the inner core while the dominant nonlinear term within the critical layer (the inertial term $\epsilon^{-3}vu_Y$) is $\mathrm{O}(\epsilon^{-3/2}\delta^2)$. The wave amplitude is thus fixed to be $\delta = \epsilon^{9/2}$ and so the critical layer expansion is

$$\begin{aligned} u &= U + \epsilon^3[\bar{u}_0 + \epsilon^{3/2}\bar{u}_1 + \epsilon^3\bar{u}_2 + \cdots],\\ v &= V + \epsilon^{9/2}[\bar{v}_0 + \epsilon^{3/2}\bar{v}_1 + \epsilon^3\bar{v}_2 + \cdots],\\ p &= P + \epsilon^3[\bar{p}_0 + \epsilon^{3/2}\bar{p}_1 + \epsilon^3\bar{p}_2 + \cdots], \end{aligned} \tag{20}$$

wherein the meanflow contributions (U, V, P) are, Taylor expanding about $x = y - y_c = 0$,

$$\begin{aligned} U &\sim U_0(y) + \epsilon^{3/2}U_1(y) + \epsilon^3 U_2(y)x_1 + \cdots\\ &\sim c_0 + \epsilon^{3/2}(b_1 Y + \tau_0) + \epsilon^3(\tau_1 Y + d_0 x_1) + \epsilon^{9/2}\left(\frac{1}{3!}b_3 Y^3 + \frac{1}{2}\tau_2 Y^2 + d_1 x_1 Y\right) + \cdots,\\ V &\sim \epsilon^6 v_{00} + \cdots,\\ P &\sim p_{00} + \epsilon^3 q_{01}x_1 + \cdots. \end{aligned} \tag{21}$$

Here the constants $b_n = U_0^{(n)}(y_c)$, $\tau_n = U_1^{(n)}(y_c)$, $d_n = U_2^{(n)}(y_c)$, etc. are determined by the oncoming boundary layer.

The critical layer expansion now proceeds as described in [26] and the many subsequent papers such as [29,31,32].

The lead order balance shows that the transverse velocity and pressure are constant within the critical level and so matching to the inner core leads to

$$\bar{p}_0 = A, \qquad \bar{v}_0 = -b_1^{-1} A_X, \tag{22}$$

while at next order the solution has $\bar{p}_1 = 0$ and, by virtue of $\bar{u}_{0Y} = 0$,

$$\bar{u}_{0X} = -\bar{v}_{1Y} = \chi A_X, \tag{23}$$

where

$$\chi = -b_1 \int_{\infty}^{y_c} \left\{ \frac{1}{[U_0 - c_0]^2} - \frac{1}{b_1^2 (y - y_c)^2} \right\} \mathrm{d}y, \tag{24}$$

is a constant determined from matching to the inner core (14). At third order in the expansion the equations which give rise to the critical level jump are obtained. These can be written as

$$L_0 \bar{u}_{1Y} + \bar{v}_0 \bar{u}_{1YY} = -(b_3 Y + \tau_2)\bar{v}_0 + \tau_1 \bar{u}_{0X}, \tag{25}$$

$$\bar{v}_{2Y} + \bar{u}_{1X} + \bar{u}_{0x_1} = 0 = \bar{p}_{2Y},$$

where the linear differential operator L_0 is

$$L_0 \equiv \frac{\partial}{\partial t_1} + c_0 \frac{\partial}{\partial x_1} + (b_1 Y + \tau_0) \frac{\partial}{\partial X} - \frac{\partial^2}{\partial Y^2}. \tag{26}$$

Matching to the inner core yields the coupling condition, using (17) and the continuity equation (25),

$$G_R^+ - G_R^- = \lim_{Y \to \infty} \bar{v}_{2Y} - \lim_{Y \to -\infty} \bar{v}_{2Y} = -\frac{\partial}{\partial X} \int\!\!\!\!\!\!- \, \bar{u}_{1Y} \, \mathrm{d}Y. \tag{27}$$

3.4. The amplitude equation

The form of the amplitude equation derived in the previous sections can be simplified considerably through a number of elementary transformations. Also, since in the following only temporal (and not spatial) modulations are of interest, all variations with respect to x_1 will be set to zero. The first transformation to be applied is used to remove the term proportional to Y from the right-hand side of (25) and is

$$\omega = \bar{u}_{1Y} - b_3 b_1^{-2} A. \tag{28}$$

Note that the term $b_3 b_1^{-2} A$ matches to the coefficient of $y - y_c$ in the solution of u_0 in the inner core. This transformation ensures that $\omega \to 0$ as $|Y| \to \infty$. The second transformation is a Galilean shift which removes the $J_2 \partial/\partial X$ term in (18) and is coupled with a change in origin of Y within the critical level

$$\widehat{X} = X - J_1^{-1} J_2 t_1, \qquad \widehat{Y} = b_1 \big(Y - J_1^{-1} J_2 + b_1^{-1} \tau_0 \big). \tag{29}$$

The final transformation involves a rescaling which allows the removal of two of the remaining constants (namely J_1 and b_3) and is

$$A = \big(2|J_1|\big)^{-1} \bar{A}, \qquad \big(X, \widehat{Y}\big) = \big(2|J_1|\big)^{-1/2} (\bar{X}, \bar{Y}), \qquad \omega = |b_3| \big(2 b_1 |J_1|\big)^{-1} \bar{\omega}. \tag{30}$$

Using these transformations in (17), (25), (27) yields the canonical problem, dropping the $\bar{\ }$'s and the subscript 1,

$$A_t + \frac{1}{\pi} \int\!\!\!\!\!\!- \, A_{\xi\xi} \frac{\mathrm{d}\xi}{X - \xi} = -\gamma \frac{\partial}{\partial X} \int\!\!\!\!\!\!- \, \omega \, \mathrm{d}Y, \tag{31}$$

$$\omega_t + Y \omega_X - A_X \omega_Y - \lambda \omega_{YY} = A_t - \mu A_X, \tag{32}$$

where γ, λ (> 0) and μ are constants and it has been assumed that $J_1 > 0$ and $b_3 < 0$. The latter condition is required for well-posedness of the linear problem as discussed in [1–3,41] while for the former changing A_t in (31) to $-A_t$ yields the equations for $J_1 < 0$.

4. Numerical method

The problem (31) and (32) is solved iteratively using second order centred differences on a nonuniform grid with a Crank–Nicolson type time marching scheme. Firstly Eq. (31) is written in the conservative form

$$A_t + F_X = 0, \tag{33}$$

where the flux F is

$$F = \gamma J + \frac{1}{\pi} \int\!\!\!\!\!\!- \int_{-\infty}^{\infty} A_\xi \frac{\mathrm{d}\xi}{X - \xi}, \tag{34}$$

with J denoting the contribution from the critical level jump. Writing $X = X_i$ $(i = 0, 2, \ldots, M + 1)$ for the X grid points and evaluating (33) at $t = (n + \frac{1}{2})\delta t$ where n is the time level and δt is the time step gives

$$A_i^{n+1} = A_i^n - \frac{2\delta t}{h_{i+1} - h_{i-1}} \big(F_{i+1/2}^{n+1/2} - F_{i-1/2}^{n+1/2}\big), \tag{35}$$

where $h_i = X_i - X_{i-1}$ and $F_{i+1/2}^{n+1/2}$ denotes and approximation to the flux at the mid-points between nodes and averaged over consecutive time levels. The contribution to the flux from the Hilbert integral is approximated using the mid-point rule which avoids the singularity at the nodal points:

$$\int\!\!\!\!\!\!- \int_{-\infty}^{\infty} A_\xi \frac{\mathrm{d}\xi}{X_i - \xi} \sim \sum_{k=0}^{N} \int\!\!\!\!\!\!- \int_{X_k}^{X_{k+1}} A_\xi \frac{\mathrm{d}\xi}{X_i - \xi} \sim \sum_{k=0}^{N} \frac{A_{k+1} - A_k}{X_i - X_{k+1/2}} = \sum_{k=1}^{N} C_{ik} A_k, \tag{36}$$

where it has been assumed that $A_0 = A_{N+1} = 0$.

To obtain values of the flux at the midpoints the quadratic interpolant

$$F_i^{\mathrm{int}}(X) = \alpha_i (X - X_i)^2 + \beta_i (X - X_i) + F_i, \tag{37}$$

is introduced where, writing $r_i = h_{i+1}/h_i$,

$$\alpha_i = \frac{r_i}{(1 + r_i) h_{i+1}^2} \big[F_{i+1} - (1 + r_i) F_i + r_i F_{i-1}\big], \tag{38}$$

$$\beta_i = \frac{1}{(1 + r_i) h_{i+1}} \big[F_{i+1} - (1 - r_i^2) F_i - r_i^2 F_{i-1}\big]. \tag{39}$$

Using this formula to obtain the values of $F_{i+1/2}$ is equivalent to using the second order difference approximation for F_X in (35) which turns out to produce grid scale instability when a disturbance crosses from a region of uniform spacing to a stretched region. This instability can be removed by ensuring that the flux $F_{i+1/2}$ used in the calculation of A_i is the same as that used in the calculation of A_{i+1}; i.e. the approximations preserve the discrete form of the integral A with respect to X. To achieve this the flux at $i + 1/2$ is calculated as the average

$$F_{i+1/2} = \frac{1}{2} \big[F_i^{\mathrm{int}}(X_{i+1/2}) + F_{i+1}^{\mathrm{int}}(X_{i+1/2})\big]. \tag{40}$$

The probable cause of this instability is the fact that on a nonuniform grid the cancellation of the singularity in the principal value integral (36) is not as accurate as it is on a uniform grid and this is likely to result in a spurious contribution to the flux. The averaging procedure described above appears to correct for this and thus stabilizes the scheme.

The second equation (32) is again solved using Crank–Nicolson for the time step and diffusion term but now, due to the change in sign of Y, the X derivative is calculated using the second order backward difference

$$\omega_X \sim \frac{\omega_{i\pm1} - s_{i\pm}^2 \omega_{i\pm2} - (1 - s_{i\pm}^2)\omega_i}{(1 - s_{i\pm})|h_{i\pm1}|}, \tag{41}$$

where $s_{i\pm} = |h_{i\pm1}/h_{i\pm2}|$ with the minus sign chosen for $Y \geqslant 0$ and the plus sign for $Y < 0$. All other derivatives are centred (with account taking of the grid stretching).

The boundary conditions for ω are applied by observing that, since ω is known at $t = 0$, the solution for ω to $\mathrm{O}(Y^{-3})$ as $|Y| \to \infty$ can be obtained by solving

$$\omega_t + Y\omega_X = A_t - \mu A_X, \tag{42}$$

which is sufficient to close the problem once the inflow condition $\omega = 0$ is applied at the lateral boundaries.

The jump across the critical level is calculated by using the asymptotic representation

$$\omega \sim q_1 Y^{-1} + q_2 Y^{-2} + \cdots, \tag{43}$$

to approximate, for large L,

$$\oint_{-\infty}^{\infty} \omega \,\mathrm{d}Y \sim \int_{-L}^{L} \omega \,\mathrm{d}Y + \frac{2q_2}{L}, \tag{44}$$

with q_2 estimated from (42) and (43) while the integral calculated using the trapezoidal rule.

The nonlinear coupled difference equations resulting from the above approximations are solved iteratively with a guess first being made for A_i^{n+1} from which the solution for ω_{ij}^{n+1} and hence the critical level jump is obtained. Using this information an updated value of A_i^{n+1} is calculated and the procedure repeated until the solution changes by less than some prescribed tolerance.

5. Results

The results described here all assume the initial condition

$$\omega \equiv 0, \qquad A = \frac{1}{10}\exp\left(-\frac{1}{4}X^2\right), \tag{45}$$

at $t = 0$. To fix matters further the constants γ and μ in (31) and (32) are chosen to be

$$\gamma = \frac{1}{3}, \qquad \mu = -\frac{5}{2}, \tag{46}$$

which ensures that a moderate range of wavenumbers (those less than $-\mu$) are unstable. The growth rate and frequency obtained from solving the linearized version of (31) and (32) are shown in Fig. 2 as a function of the wavenumber α.

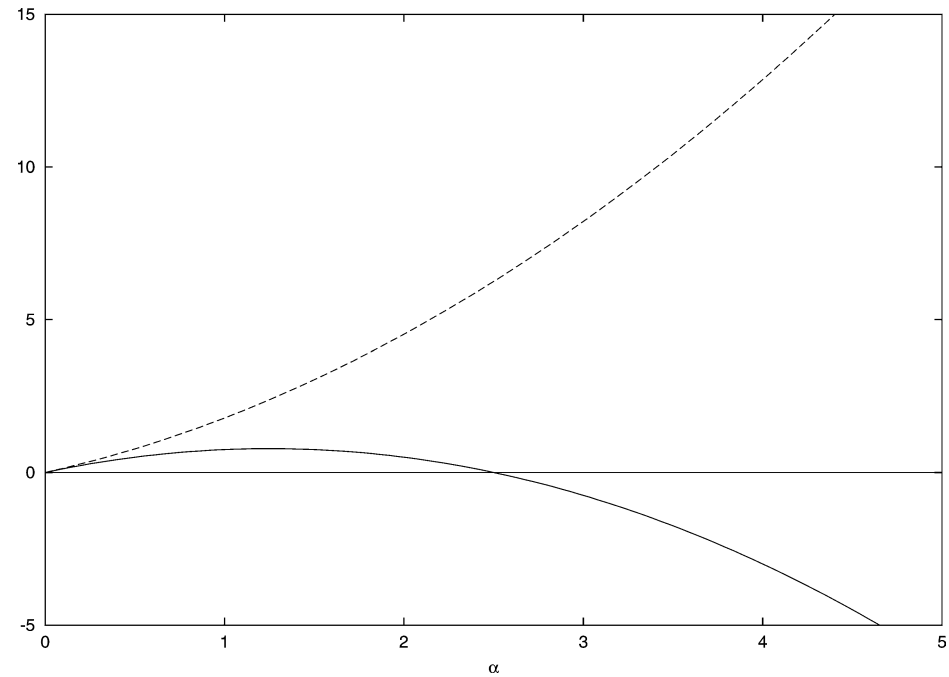

Fig. 2. The linear growth rate predicted from (31) and (32). Here the α is the wavenumber, the solid line is the growth rate and the broken line is the frequency.

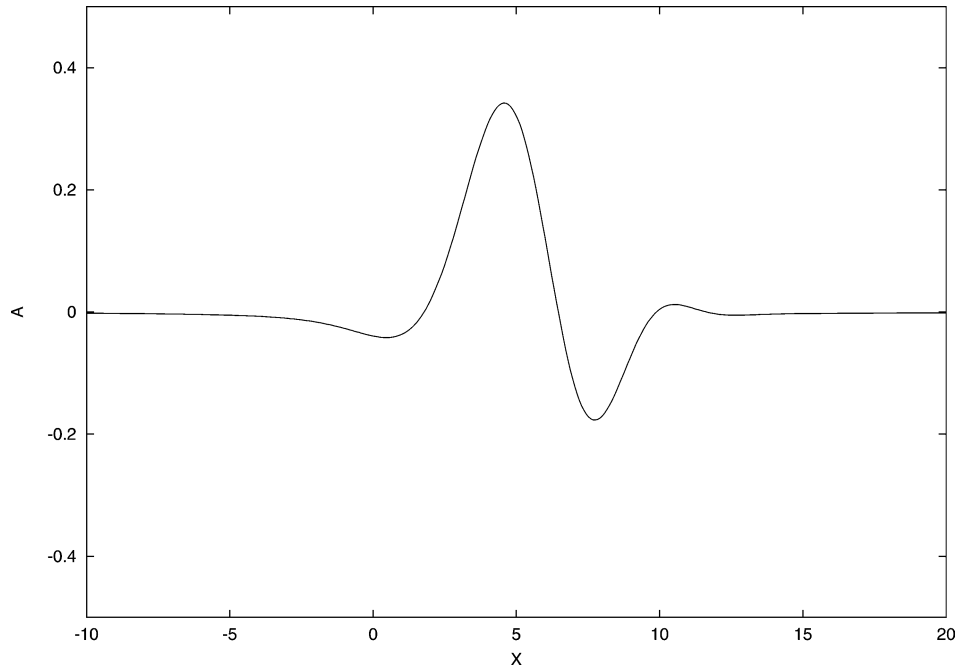

(a)

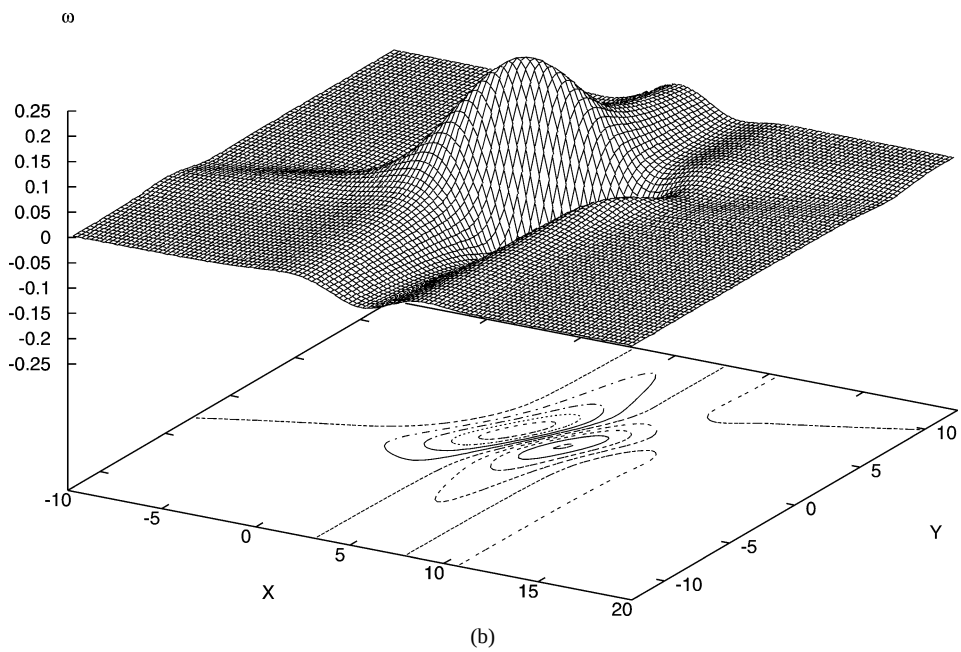

(b)

Fig. 3. The solution at $t = 2.5$ (a) is the amplitude function A, (b) is ω and (c) is S. Note that the contours for S can be read off the Y axis by virtue of the initial condition

In the following, as well as shown solutions for A and ω, it will be useful to also consider the evolution of a scalar quantity S satisfying

$$S_t + Y S_X - A_X S_Y = 0, \tag{47}$$

with

$$S = Y \quad \text{at } t = 0. \tag{48}$$

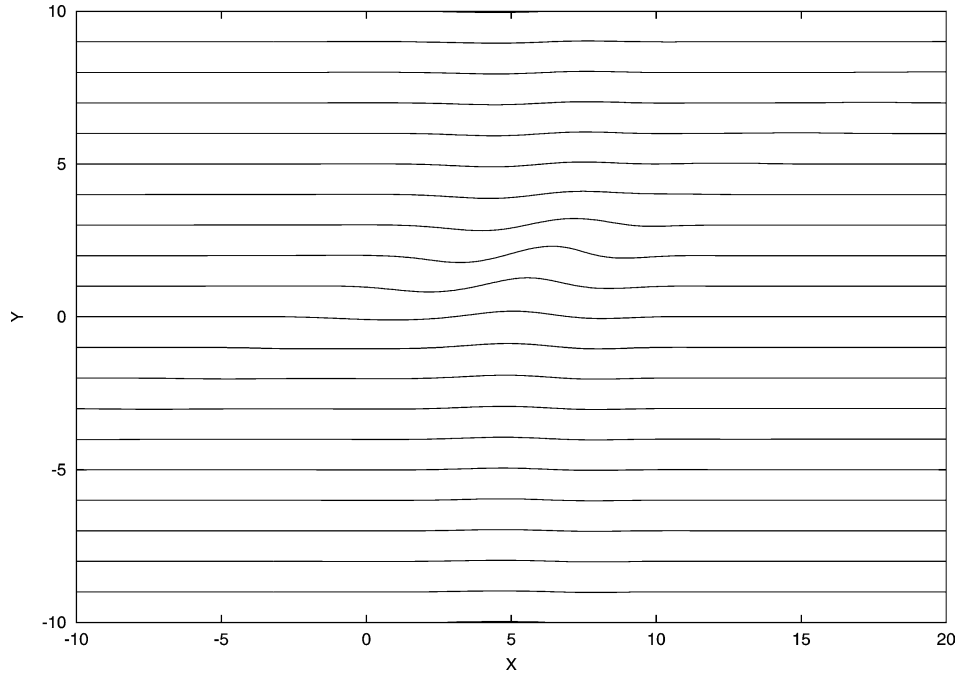

(c)

Fig. 3. Continued.

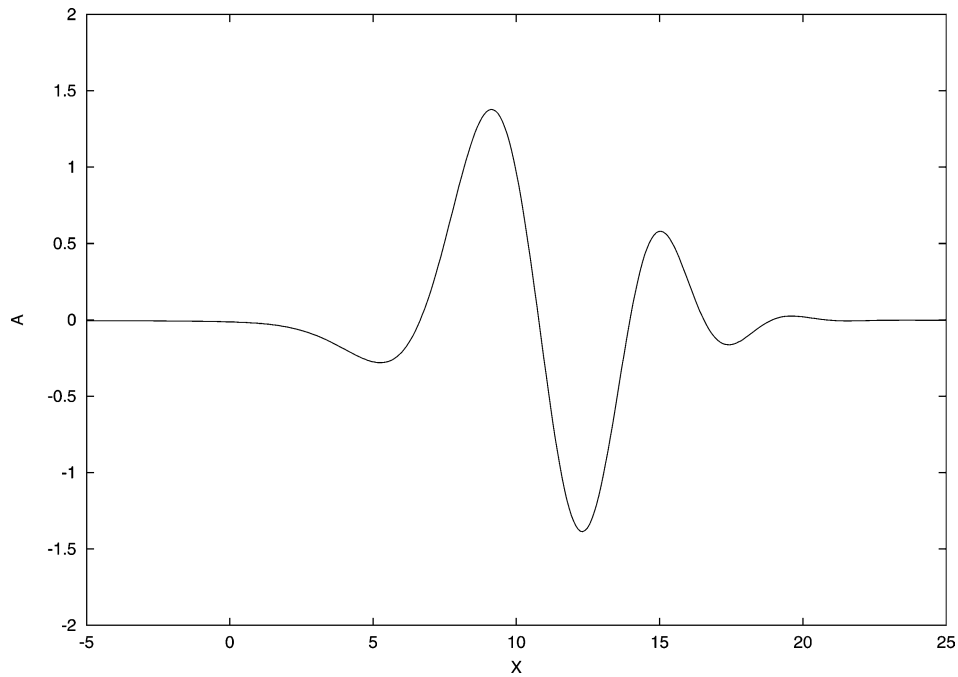

(a)

Fig. 4. As Fig. 3 but for $t = 5$.

The advantage of this quantity over that of the streamfunction $\frac{1}{2}Y^2 + A$ is that, due to the fact that S remains constant on a particle path, the lines of constant S will mimic the use of gas bubbles/dye as is often used in flow visualization experiments.

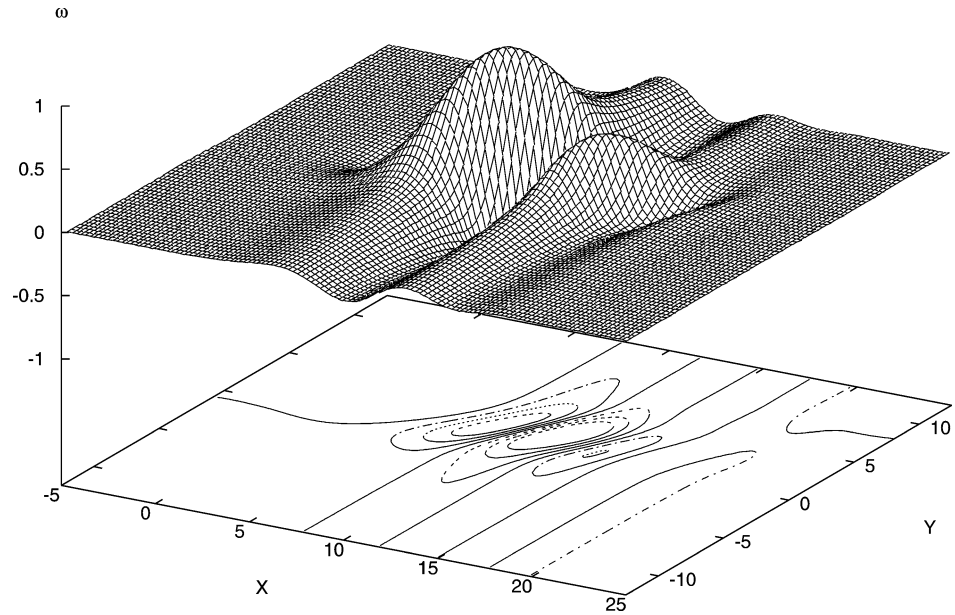

(b)

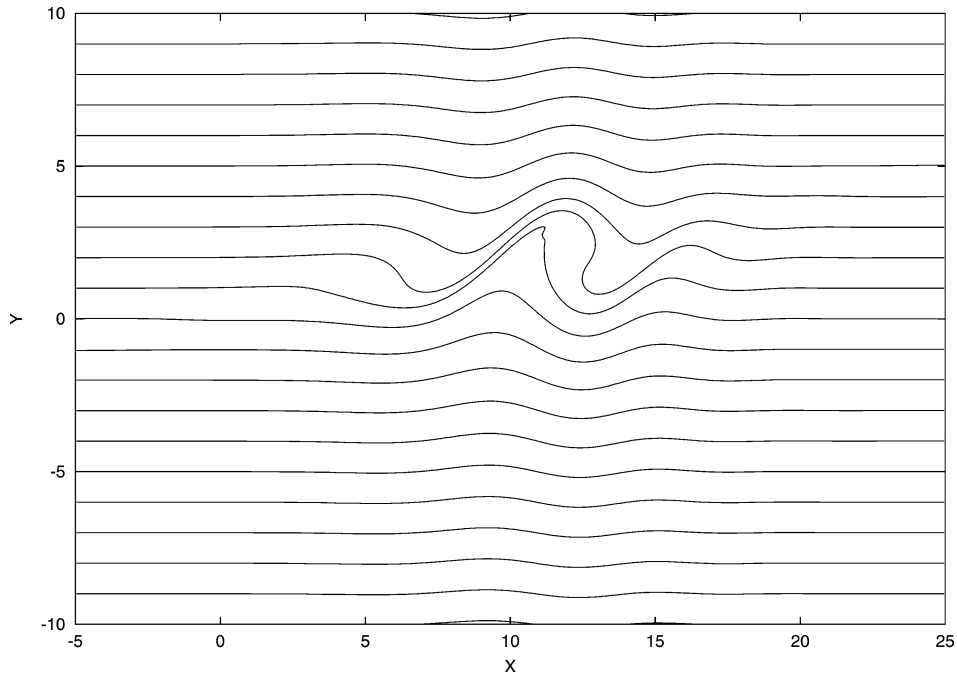

(c)

Fig. 4. Continued.

In the results described here a uniform grid of spacing 0.08 in X was used for $-25 \leqslant X \leqslant 35$ with the grid then slowly stretched until $X \sim 80$ while in the Y direction the grid was uniform, with spacing 0.0833, for $|Y| \leqslant 12.5$ with stretching up to $Y \sim 31$. This resulted in a grid which was 1000×600. The large value of the convection velocity at the edge of the domain requires a small time step, here chosen to be 0.0025, to ensure that the Courant number is less that unity. To test the convergence of the numerics a simulation was also performed at a higher resolution of 1500×1000 which showed no discernable differences.

In the following the detailed solutions will be described for $\lambda = 1$ with a discussion of the effects of different values summarized later. The results for $t = 2.5$ are shown in Fig. 3 at which point the dynamics are still purely linear in nature.

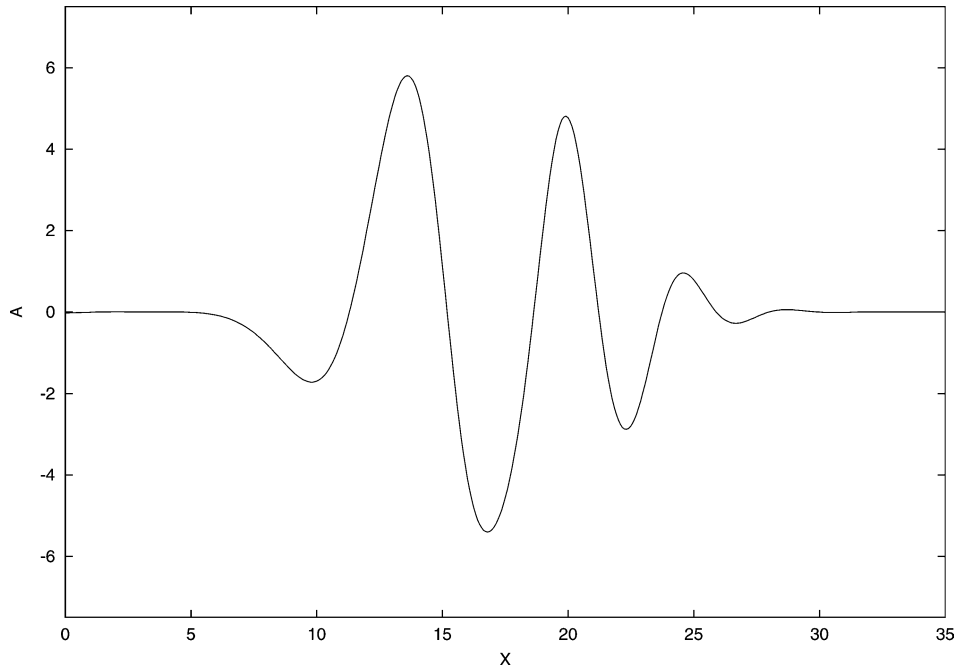

(a)

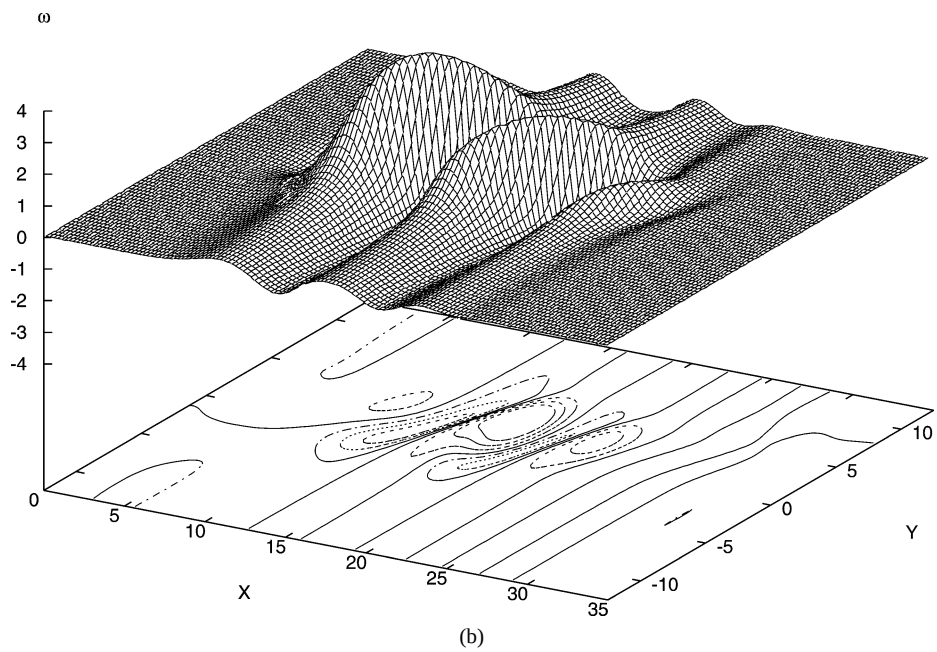

(b)

Fig. 5. As Fig. 3 but for $t = 7.5$.

As noted in the previous section the integral of A with respect to X must remain constant and so the negative values of A are required by the solution in order to balance the growth and dispersion of the spot disturbance.

In Fig. 4 the solution at the later time $t = 5$ is shown. At this point the first signs of nonlinearity are coming into effect, although the solution is still very much linear at this stage (see discussion below), and in particular the rolling up of the critical layer vortex can be clearly seen in Fig. 4(c). At the later time $t = 7.5$ shown in Fig. 5 the rapid nonlinear growth of the disturbance is clearly visible with the formation of multiple maxima and minima in the pressure A. The viscosity and

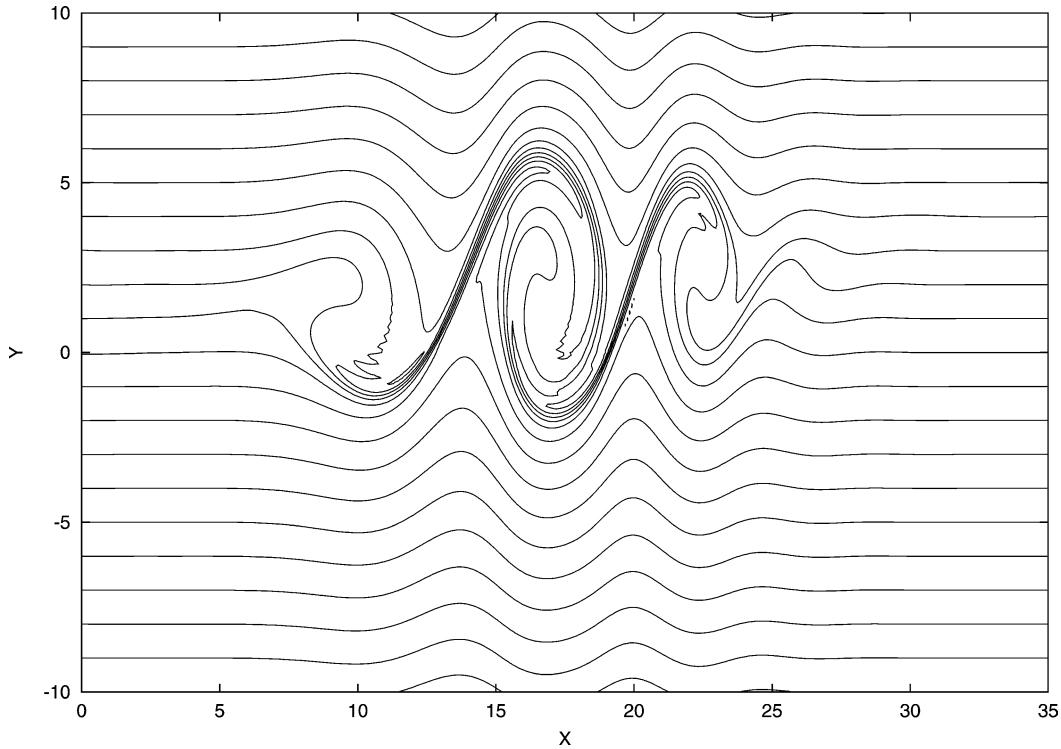

(c)

Fig. 5. Continued.

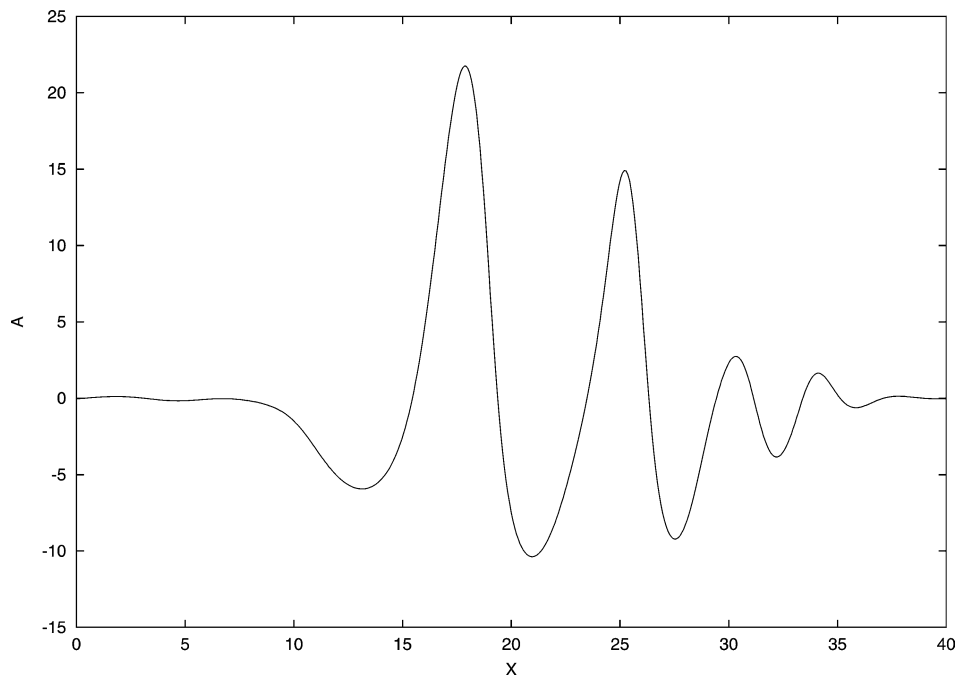

(a)

Fig. 6. As Fig. 3 but for $t = 10$.

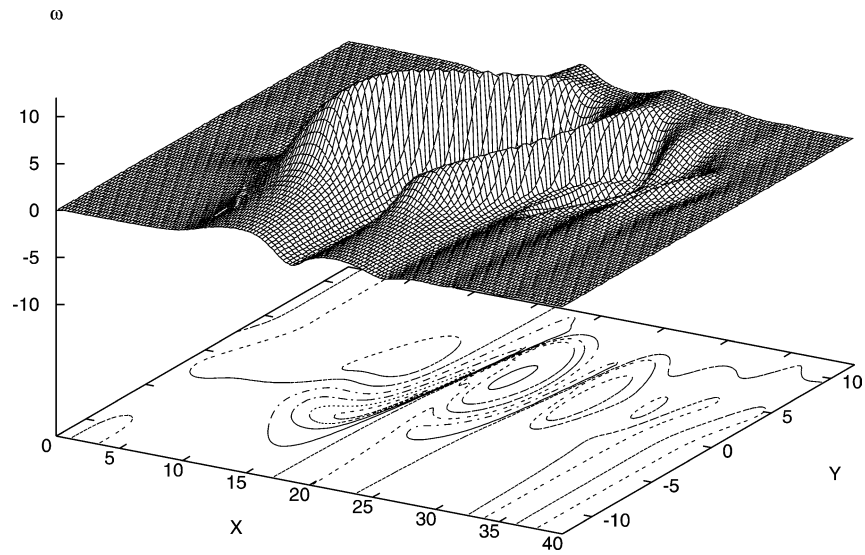

(b)

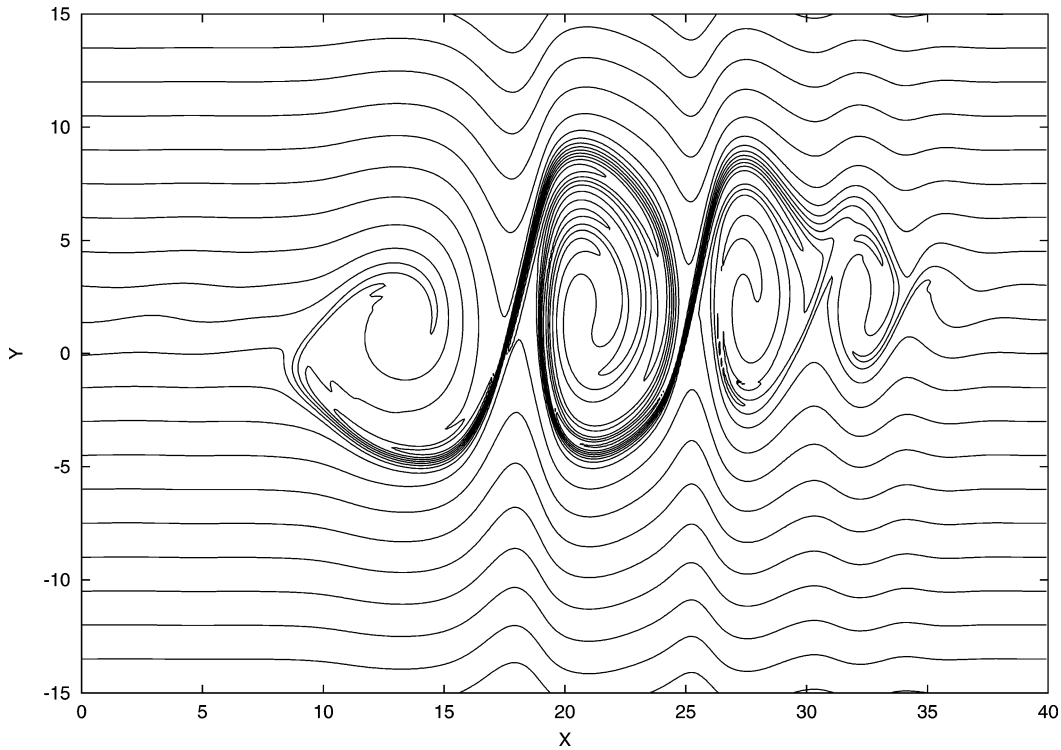

(c)

Fig. 6. Continued.

nonlinearity within the critical layer appears to only slightly decrease the growth of the disturbance. The resulting formation secondary vortices within the critical layer can clearly seen in the contours of S.

At $t = 10$ the growth of A has continued (Fig. 6) and there is no sign of either finite amplitude equilibration nor break-up due to the formation of a singularity. The solution has also become more oscillatory with the resulting formation and growth of smaller vortices becoming more evident. These multiple vortices hint at a tendency to form a periodic array of large amplitude

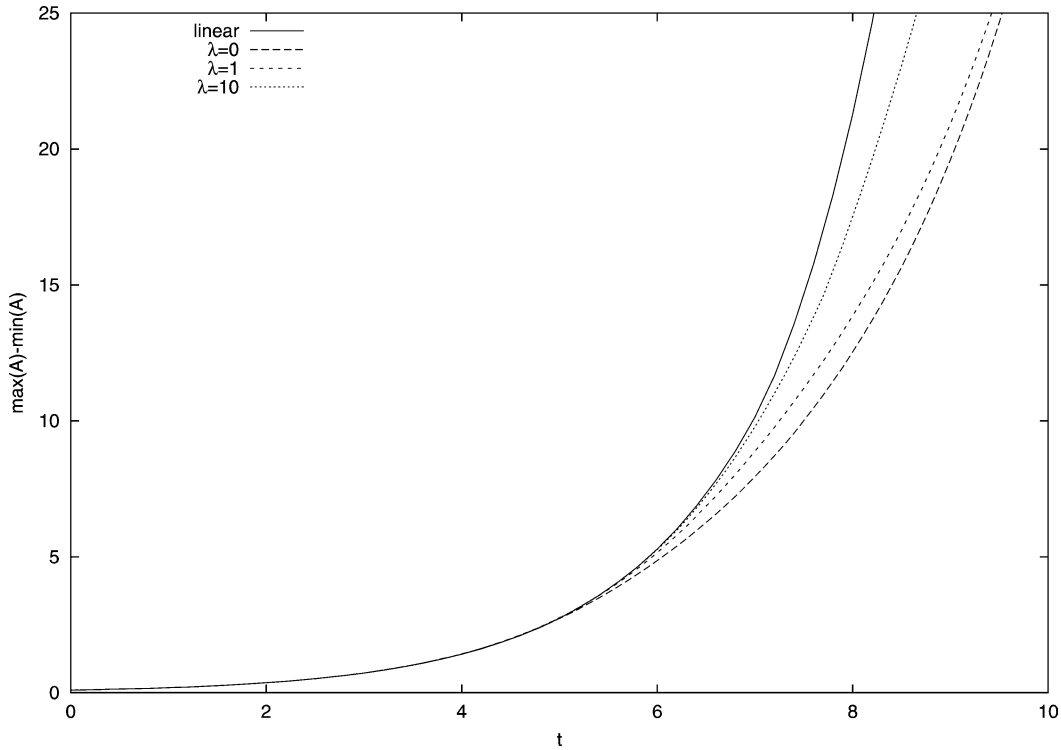

Fig. 7. The difference between then maximum and minimum values of A as a function of time for different values of the viscosity parameter λ. The solid line is the prediction of the linearized problem.

vortices as $t \to \infty$. The *wavelength* of the disturbance appears to be close to that predicted from linear theory (see Fig. 2) for the fastest growing wave.

Since the solutions for different values of the critical layer diffusion parameter λ show similar behaviour to the results already described the effects of viscosity (and nonlinearity) can best be described by considering the difference between the largest and smallest values of A as a function of time for different values of λ as shown in Fig. 7. Also shown in this graph is the growth predicted by the linearized equations which clearly shows that all the nonlinear solutions possess growth rates smaller than that predicted by linear theory. Surprisingly these results also indicate that the more viscous solutions have the greater growth rates which at first sight appears to be counter intuitive. The larger growth of the viscous solutions appear to arise from the fact that although the maximum values of ω are smaller within the critical level for the larger values of λ the spreading out of the disturbance in the transverse (Y) direction due to dissipation increases the value of the integral of ω across the critical layer and hence increases the magnitude of the jump. This result is implied in the asymptotic analysis of [31] which shows, following the work of Brown and Stewartson [42], that the critical layer splits into two as $\lambda \to \infty$ with the inner critical layer buffered by an outer diffusion layer. Another striking feature of this graph is the indication that the solution is actually behaving linearly for much of the evolution, up to around $t = 5$, even when the amplitude function A has become relatively large and so cannot be expected to agree with the linear theory which requires $|A| \ll 1$.

6. Discussion

The results described in the previous section show important differences to the periodic case studied by [30] and [31]. Firstly the results presented here show only a small difference between the inviscid ($\lambda = 0$) and viscous ($\lambda = 1$) solutions while in the two cited papers it was found that the inviscid solution would undergo finite amplitude equilibration and that viscosity led to algebraic growth of A. Another important difference is that the nonlinear growth, although smaller than that predicted by linear theory, appears to remain exponential rather than simply algebraic.

This final point along with the question of the ultimate fate of the disturbance on time scales longer than those considered here deserves further study. In particular an analysis similar to that started in [31] and completed in [32] would be of particular

interest. Such a study would also clarify the relationship of the present work to that of Li et al. [43]. The simplicity of the present problem compared to the three-dimensional work of [2,3] should make such an approach analytically viable.

The problem of matching back to an initially linearly growing disturbance as $t \to -\infty$, which is not possible in either the present work or that of the preceding papers [1–3,41], also needs some consideration. As described in these papers the linearized problem is ill-posed[3] in $t < 0$ in the case of physical interest $b_3 < 0$ which results in a well-posed problem for $t > 0$. In order to obtain a well-posed problem in $t < 0$ it is necessary to have $b_3 > 0$ which results in an ill-posed problem for $t > 0$. A study of the receptivity problem for Rayleigh waves, to which this problem is fundamentally related, has recently been started by Smith and Timoshin [44] who show how a linear disturbance can be followed from its initiation at a pressure minimum to the formation of a *group-velocity* critical layer and subsequent nonlinear evolution. How such a matching could be performed for the current problem is at present an open question.

Acknowledgements

The author would like to thank an anonymous referee for useful comments which helped to clarify the presentation of this paper and also for reminding him of the work of Gaster [11] and Kendall [14].

References

[1] D.J. Savin, F.T. Smith, T. Allen, Transition of free disturbances in inflectional flow over an isolated surface roughness, Proc. R. Soc. Lond. Ser. A 455 (1999) 491–541.
[2] T. Allen, S.N. Brown, F.T. Smith, An initial-value problem for fully three-dimensional inflectional boundary layer flows, Theoret. Comput. Fluid Dynamics 12 (1998) 131–148.
[3] T. Allen, The evolution of free-disturbances on an initially two-dimensional inflectional boundary layer flow, Q. J. Mech. Appl. Math 57 (2004) 115–136.
[4] F.T. Smith, Laminar flow over a small hump on a flat plate, J. Fluid Mech. 57 (1973) 803–824.
[5] F.T. Smith, P.W.M. Brighton, P.S. Jackson, J.C.R. Hunt, On boundary layer flow past two-dimensional obstacles, J. Fluid Mech. 113 (1981) 123–152.
[6] O.R. Tutty, S.J. Cowley, On the stability and numerical solution of the unsteady interactive boundary layer equations, J. Fluid Mech. 168 (1986) 431–456.
[7] F.T. Smith, R.J. Bodonyi, On short-scale inviscid instabilities in the flow past surface mounted obstacles and other non-parallel motions, Aeron. J. R. Aeron. Soc., June/July (1985) 205–212.
[8] K. Stewartson, Multi-structural boundary layers on flat plates and related bodies, Adv. Appl. Mech. 14 (1974) 145–239.
[9] F.T. Smith, On the high Reynolds number theory of laminar flows, IMA J. Appl. Math. 28 (1982) 207–281.
[10] C.J. Chapman, M.R.E. Proctor, Nonlinear Rayleigh–Bènard convection between poorly conducting boundaries, J. Fluid Mech. 101 (1980) 759–782.
[11] M. Gaster, A theoretical model of a wave packet in the boundary layer on a flat plate, Proc. R. Soc. Lond. Ser. A 347 (1975) 271–289.
[12] M. Gaster, I. Grant, An experimental investigation of the formation and development of a wave packet in a laminar boundary layer, Proc. R. Soc. Lond. Ser. A 347 (1975) 253–269.
[13] P.S. Klebanoff, K.D. Tidstrom, Mechanism by which a two-dimensional roughness element induces boundary layer transition, Phys. Fluids 15 (1972) 1173–1188.
[14] J.M. Kendall, Laminar boundary layer velocity distortion by surface roughness, effect upon stability, AIAA paper 81-0195.
[15] N. Gregory, W.S. Walker, The effect on transition of isolated surface excrescences in the boundary layer, Tech. Rep. 2779, Aero. Res. Council R&M, 1956.
[16] Y.S. Kachanov, Three-dimensional instabilities in boundary layers, in: Proc. Symp. on Transitional Boundary Layers in Aeronautics, Amsterdam, Netherlands, Springer-Verlag, Berlin, 1995, pp. 55–70.
[17] P.J. Mason, B.R. Morton, Trailing vortices in the wakes of surface-mounted obstacles, J. Fluid Mech. 175 (1987) 247–293.
[18] W.S. Saric, M.S. Reibert, R.H. Radeztsky, R.B. Carillo, Nonlinear stability, saturation, and transition in swept-wing flows, in: Proc. Symp. on Transitional Boundary Layers in Aeronautics, Amsterdam, Netherlands, Springer-Verlag, Berlin, 1995, pp. 125–135.
[19] M.A. Zanchetta, R. Hillier, Blunt cone transition at hypersonic speeds: the transition reversal regime, in: Proc. Symp. on Transitional Boundary Layers in Aeronautics, Amsterdam, Netherlands, Springer-Verlag, Berlin, 1995, pp. 433–440.
[20] M.V. Morkovin, On roughness-induced transition: facts, views, and speculations, in: M.Y. Hussaini, R.G. Voigt (Eds.), Instability and Transition, vol. 1, Springer-Verlag, New York, 1990, pp. 281–295.
[21] M. Van Dyke, An Album of Fluid Motion, Parabolic Press, Palo Alto, CA, 1982.

[3] The ill-posedness arises due to the fact that the exponentially decaying (in time) waves with large wavenumber are exponentially growing for $t \to -\infty$.

[22] M.E. Goldstein, S.-W. Choi, Nonlinear evolution of interacting oblique waves on two-dimensional shear layers, J. Fluid Mech. 207 (1989) 73–96.
[23] X. Wu, S.J. Cowley, On the nonlinear evolution of instability modes in unsteady shear layers: The stokes layer as a paradigm, Q. J. Mech. Appl. Math. 48 (1995) 159–188.
[24] X. Wu, S.S. Lee, S.J. Cowley, On the weakly nonlinear three-dimensional instability of shear layers to pairs of oblique waves: the stokes layer as a paradigm, J. Fluid Mech. 253 (1993) 681–721.
[25] F.J. Hickernell, Time-dependent critical layers in shear flows on the beta-plane, J. Fluid Mech. 142 (1984) 431–449.
[26] K. Stewartson, The evolution of the critical layer of a Rossby wave, Geophys. Astrophys. Fluid Dynamics 9 (1978) 185–200.
[27] K. Stewartson, Marginally stable inviscid flows with critical layers, IMA J. Appl. Math. 27 (1981) 133–175.
[28] S.A. Maslowe, Critical layers in shear flows, Annu. Rev. Fluid Mech. 18 (1986) 405–432.
[29] M.E. Goldstein, P.A. Durbin, S.J. Leib, Roll-up of vorticity in adverse-pressure-gradient boundary layers, J. Fluid Mech. 183 (1987) 325–342.
[30] M.E. Goldstein, S.J. Leib, Nonlinear roll-up of externally excited free shear layer, J. Fluid Mech. 191 (1988) 481–515.
[31] M.E. Goldstein, L.S. Hultgren, Nonlinear spatial evolution of an externally excited instability wave in a free shear layer, J. Fluid Mech. 197 (1988) 295–330.
[32] L.S. Hultgren, Nonlinear spatial equilibration of an externally excited instability wave in a free shear layer, J. Fluid Mech. 236 (1992) 635–664.
[33] K. Stewartson, On the flow near the trailing edge of a flat plate II, Mathematika 16 (1) (1969) 106–121.
[34] A.F. Messiter, Boundary-layer flow near the trailing edge of a flat plate, SIAM J. Appl. Math. 18 (1) (1970) 241–257.
[35] F.T. Smith, Finite-time break-up can occur in any unsteady interacting boundary layer, Mathematika 35 (1988) 256–273.
[36] V.J. Peridier, F.T. Smith, J.D.A. Walker, Vortex induced boundary-layer separation. Part 2. unsteady interacting boundary-layer theory, J. Fluid Mech. 232 (1991) 133–165.
[37] J.M. Hoyle, F.T. Smith, J.D.A. Walker, On sublayer eruption and vortex formation, Comput. Phys. Commun. 65 (1991) 151–157.
[38] K.W. Cassel, F.T. Smith, J.A. Walker, The onset of instability in unsteady boundary-later separation, J. Fluid Mech. 315 (1996) 223–256.
[39] R.S. Johnson, A Modern Introduction to the Mathematical Theory of Water Waves, Cambridge University Press, 1997.
[40] P.G. Drazin, W.H. Reid, Hydrodynamic Stability, Cambridge University Press, 1981.
[41] S.N. Brown, F.T. Smith, Spot concentrations of large-amplitude disturbances laminar boundary layers, Q. J. Mech. Appl. Math. 52 (1999) 269–281.
[42] S.N. Brown, K. Stewartson, The evolution of the critical layer of a Rossby wave. Part II, Geophys. Astrophys. Fluid Dynamics 10 (1978) 1–24.
[43] L. Li, J.D.A. Walker, R.I. Bowles, F.T. Smith, Short-scale break-up in unsteady interactive layers: local development of normal pressure gradients and vortex wind-up, J. Fluid Mech. 374 (1998) 335–378.
[44] F.T. Smith, S.N. Timoshin, On ‘spot’ evolution under an adverse pressure gradient, J. Fluid Mech. 430 (2001) 169–207.